

ASYMPTOTICALLY EXACT A POSTERIORI ERROR ESTIMATES OF EIGENVALUES BY THE CROUZEIX-RAVIART ELEMENT AND ENRICHED CROUZEIX-RAVIART ELEMENT

JUN HU AND LIMIN MA

ABSTRACT. Two asymptotically exact a posteriori error estimates are proposed for eigenvalues by the nonconforming Crouzeix–Raviart and enriched Crouzeix–Raviart elements. The main challenge in the design of such error estimators comes from the nonconformity of the finite element spaces used. Such nonconformity causes two difficulties, the first one is the construction of high accuracy gradient recovery algorithms, the second one is a computable high accuracy approximation of a consistency error term. The first difficulty was solved for both nonconforming elements in a previous paper. Two methods are proposed to solve the second difficulty in the present paper. In particular, this allows the use of high accuracy gradient recovery techniques. Further, a post-processing algorithm is designed by utilizing asymptotically exact a posteriori error estimators to construct the weights of a combination of two approximate eigenvalues. This algorithm requires to solve only one eigenvalue problem and admits high accuracy eigenvalue approximations both theoretically and numerically.

Keywords. eigenvalue problems, nonconforming elements, asymptotically exact a posteriori error estimates

AMS subject classifications. 65N30, 73C02.

1. INTRODUCTION

Asymptotically exact a posteriori error estimators are widely used to improve accuracy of approximations. A posteriori error estimators were first proposed by Babuška and Rheinboldt in 1978 [2]. Since then, some important branches of a posteriori error estimators have been developed, such as residual type a posteriori error estimators [1, 4, 6, 7] and recovery type a posteriori error estimators [3, 5, 17, 22, 24, 25]. For eigenvalues of the Laplacian operator by the conforming linear element, asymptotically exact a posteriori error estimates were proposed and analyzed in [18]. These error estimators play an important role in improving the accuracy of eigenvalues to a remarkable fourth order. For this conforming element, errors of eigenvalues can be decomposed into the square of the energy norm of errors of eigenfunctions and a higher order term. Asymptotically exact a posteriori error estimators follow directly from this crucial fact and an application

The authors were supported by NSFC projects 11625101, 91430213 and 11421101.

of high accuracy gradient recovery techniques, such as polynomial preserving recovery techniques (PPR for short hereinafter) in [23], Zienkiewicz-Zhu superconvergence patch recovery techniques (SPR for short hereinafter) in [26] and the superconvergent cluster recovery method in [16].

As for nonconforming elements, errors of eigenvalues are composed of the energy norm of errors of corresponding eigenfunctions, an extra consistency term and a higher order term. The nonconformity causes two major difficulties, the first one is the construction of high accuracy gradient recovery algorithms, the second one is a computable high accuracy approximation to the consistency error term. A previous paper [13] analyzes the optimal superconvergence results for both the nonconforming Crouzeix-Raviart (CR for short hereinafter) element and the enriched Crouzeix-Raviart (ECR for short hereinafter) element. It offers a computable high accuracy approximation to the energy norm of eigenfunctions. The aforementioned consistency error term requires to approximate eigenfunctions themselves with high accuracy, not gradients of eigenfunctions any more. The fact that there exist no such function recovery techniques in literature causes the second difficulty for nonconforming elements.

Two types of asymptotically exact a posteriori error estimators of eigenvalues are designed for the nonconforming CR element and the ECR element. The main idea here is to turn this function recovery problem into a high accuracy gradient recovery problem. The first type of a posteriori error estimators employs a commuting interpolation of eigenfunctions, and the second type makes use of a conforming interpolation of eigenfunctions. Both types of asymptotically exact a posteriori error estimators require the high accuracy gradient recovery technique for the nonconforming CR element and the ECR element. The first design of asymptotically exact a posteriori error estimates is much easier to implement but requires a commutable interpolation, while the other one applies for more general nonconforming elements as long as the corresponding discrete space contains a conforming subspace. Although both error estimates achieve the same theoretical accuracy, experiments indicate even higher accuracy for the first type of error estimates when eigenfunctions are smooth enough. While the second one admits much better experimental performance when eigenfunctions are singular.

An additional technique for high precision eigenvalues is to combine two approximate eigenvalues by a weighted-average [11]. The accuracy of the resulting combining eigenvalues depends on the accuracy of the weights. In [11], two finite elements are employed to solve eigenvalue problems on two meshes with one element producing upper bounds of eigenvalues and the other one producing lower bounds. The main idea there is to design approximate weights through these four resulting discrete eigenvalues. This algorithm is verified to be quite efficient by experiments.

By use of the aforementioned asymptotically exact a posteriori error estimators, a new post-processing algorithm is proposed and analyzed to improve the accuracy of eigenvalues. Given lower bounds of eigenvalues and the corresponding nonconforming approximate eigenfunctions, an application of the average-projection method [10] to these eigenfunctions yields conforming approximate eigenfunctions. By [10], Rayleigh quotients of such conforming eigenfunctions are asymptotical upper bounds of eigenvalues.

The new algorithm combines the lower bounds and the upper bounds of eigenvalues by a weighted-average. The weights here are designed from the corresponding asymptotically exact a posteriori error estimators. The resulting combining eigenvalues are proved to admit higher accuracy both theoretically and experimentally. It needs to point out that only one discrete eigenvalue problem needs to be solved in this new algorithm.

The remaining paper is organized as follows. Section 2 presents second order elliptic eigenvalue problems and some notations. Section 3 establishes and analyzes asymptotically exact a posteriori error estimators of eigenvalues by the nonconforming CR element and the ECR element. Section 4 proposes two post-processing algorithms to approximate eigenvalues with high accuracy. Section 5 presents some numerical tests.

2. NOTATIONS AND PRELIMINARIES

2.1. Notations. We first introduce some basic notations. Given a nonnegative integer k and a bounded domain $\Omega \subset \mathbb{R}^2$ with boundary $\partial\Omega$, let $W^{1,\infty}(\Omega, \mathbb{R})$, $H^k(\Omega, \mathbb{R})$, $\|\cdot\|_{k,\Omega}$ and $|\cdot|_{k,\Omega}$ denote the usual Sobolev spaces, norm, and semi-norm, respectively. And $H_0^1(\Omega, \mathbb{R}) = \{u \in H^1(\Omega, \mathbb{R}) : u|_{\partial\Omega} = 0\}$. Denote the standard $L^2(\Omega, \mathbb{R})$ inner product and $L^2(K, \mathbb{R})$ inner product by (\cdot, \cdot) and $(\cdot, \cdot)_{0,K}$, respectively.

Suppose that $\Omega \subset \mathbb{R}^2$ is a bounded polygonal domain covered exactly by a shape-regular partition \mathcal{T}_h into simplices. Let element K have vertices $\mathbf{p}_i = (p_{i1}, p_{i2})$, $1 \leq i \leq 3$ oriented counterclockwise, and corresponding barycentric coordinates $\{\phi_i\}_{i=1}^3$. Denote $\{e_i\}_{i=1}^3$ the edges of element K , and $\{\mathbf{t}_i\}_{i=1}^3$ the unit tangent vectors with counterclockwise orientation. Denote the column vectors $\mathbf{e}_1 = (1, 0)^T$ and $\mathbf{e}_2 = (0, 1)^T$.

Let $|K|$ denote the volume of element K and $|e|$ the length of edge e . Let h_K denote the diameter of element $K \in \mathcal{T}_h$ and $h = \max_{K \in \mathcal{T}_h} h_K$. Denote the set of all interior edges and boundary edges of \mathcal{T}_h by \mathcal{E}_h^i and \mathcal{E}_h^b , respectively, and $\mathcal{E}_h = \mathcal{E}_h^i \cup \mathcal{E}_h^b$. For any interior edge $e = K_e^1 \cap K_e^2$, we denote the element with larger global label by K_e^1 , the one with smaller global label by K_e^2 . Let $\{\cdot\}$ and $[\cdot]$ be averages and jumps of piecewise functions over edge e , namely

$$\{v\}|_e := \frac{1}{2}(v|_{K_e^1} + v|_{K_e^2}), \quad [v]|_e := v|_{K_e^1} - v|_{K_e^2}$$

for any piecewise function v . For $K \subset \mathbb{R}^2$, $r \in \mathbb{Z}^+$, let $P_r(K)$ be the space of all polynomials of degree not greater than r on K . Denote the second order derivatives $\frac{\partial^2 u}{\partial x_i \partial x_j}$ by $\partial_{x_i x_j} u$, $1 \leq i, j \leq 2$, the piecewise gradient operator and the piecewise Hessian operator by ∇_h and ∇_h^2 , respectively.

Throughout the paper, a positive constant independent of the mesh size is denoted by C , which refers to different values at different places.

2.2. Eigenvalue problems for nonconforming elements. On a domain $\Omega \subset \mathbb{R}^2$ with Lipschitz boundary, we consider a model eigenvalue problem of finding $(\lambda, u) \in \mathbb{R} \times V$ such that $\|u\|_{0,\Omega} = 1$ and

$$(2.1) \quad a(u, v) = \lambda(u, v) \quad \text{for any } v \in V,$$

where $V := H_0^1(\Omega, \mathbb{R})$. The bilinear form $a(w, v) := \int_{\Omega} \nabla w \cdot \nabla v \, dx$ is symmetric, bounded, and coercive, namely for any $w, v \in V$,

$$a(w, v) = a(v, w), \quad |a(w, v)| \leq C \|w\|_{1, \Omega} \|v\|_{1, \Omega}, \quad \|v\|_{1, \Omega}^2 \leq Ca(v, v).$$

The eigenvalue problem (2.1) has a sequence of eigenvalues

$$0 < \lambda_1 \leq \lambda_2 \leq \lambda_3 \leq \dots \nearrow +\infty,$$

and the corresponding eigenfunctions u_1, u_2, u_3, \dots , with

$$(u_i, u_j) = \delta_{ij} \quad \text{with } \delta_{ij} = \begin{cases} 0 & i \neq j \\ 1 & i = j \end{cases}.$$

Let V_h be a nonconforming finite element approximation to V over \mathcal{T}_h . The corresponding finite element approximation of (2.1) is to find $(\lambda_h, u_h) \in \mathbb{R} \times V_h$, such that $\|u_h\|_{0, \Omega} = 1$ and

$$(2.2) \quad a_h(u_h, v_h) = \lambda_h(u_h, v_h) \quad \text{for any } v_h \in V_h,$$

with the discrete bilinear form $a_h(w_h, v_h)$ defined elementwise as

$$a_h(w_h, v_h) := \sum_{K \in \mathcal{T}_h} \int_K \nabla_h w_h \cdot \nabla_h v_h \, dx.$$

Let $N = \dim V_h$. Suppose that $\|\cdot\|_h := a_h(\cdot, \cdot)^{1/2}$ is a norm over the discrete space V_h , the discrete problem (2.2) admits a sequence of discrete eigenvalues

$$0 < \lambda_{1,h} \leq \lambda_{2,h} \leq \lambda_{3,h} \leq \dots \nearrow \lambda_{N,h},$$

and the corresponding eigenfunctions $u_{1,h}, u_{2,h}, \dots, u_{N,h}$, with $(u_{i,h}, u_{j,h}) = \delta_{ij}$.

We consider the following two nonconforming elements: the CR element and the ECR element.

- The CR element space over \mathcal{T}_h is defined in [8] by

$$V_{\text{CR}} := \left\{ v \in L^2(\Omega, \mathbb{R}) \mid v|_K \in P_1(K) \text{ for any } K \in \mathcal{T}_h, \int_e [v] \, ds = 0 \text{ for any } e \in \mathcal{E}_h^i, \int_e v \, ds = 0 \text{ for any } e \in \mathcal{E}_h^b \right\}.$$

Moreover, we define the canonical interpolation operator $\Pi_{\text{CR}} : H^1(\Omega, \mathbb{R}) \rightarrow V_{\text{CR}}$ as follows:

$$(2.3) \quad \int_e \Pi_{\text{CR}} v \, ds = \int_e v \, ds \quad \text{for any } e \in \mathcal{E}_h, v \in H^1(\Omega, \mathbb{R}).$$

Denote the approximate eigenpair of (2.2) in the nonconforming space V_{CR} by $(\lambda_{\text{CR}}, u_{\text{CR}})$ with $\|u_{\text{CR}}\|_{0, \Omega} = 1$.

- The ECR element space over \mathcal{T}_h is defined in [9] by

$$V_{\text{ECR}} := \left\{ v \in L^2(\Omega, \mathbb{R}) \mid v|_K \in \text{ECR}(K) \text{ for any } K \in \mathcal{T}_h, \int_e [v] ds = 0 \text{ for any } e \in \mathcal{E}_h^i, \right. \\ \left. \int_e v ds = 0 \text{ for any } e \in \mathcal{E}_h^b \right\}.$$

with $\text{ECR}(K) = P_1(K) + \text{span}\{x_1^2 + x_2^2\}$. Define the canonical interpolation operator $\Pi_{\text{ECR}} : H^1(\Omega, \mathbb{R}) \rightarrow V_{\text{ECR}}$ by

$$(2.4) \quad \int_e \Pi_{\text{ECR}} v ds = \int_e v ds, \quad \int_K \Pi_{\text{ECR}} v dx = \int_K v dx \quad \forall e \in \mathcal{E}_h, K \in \mathcal{T}_h.$$

Denote the approximate eigenpair of (2.2) in the nonconforming space V_{ECR} by $(\lambda_{\text{ECR}}, u_{\text{ECR}})$ with $\|u_{\text{ECR}}\|_{0,\Omega} = 1$.

It follows from the theory of nonconforming eigenvalue approximations in [9] that

$$(2.5) \quad |\lambda - \lambda_{\text{CR}}| + \|u - u_{\text{CR}}\|_{0,\Omega} + h^s \|\nabla_h(u - u_{\text{CR}})\|_{0,\Omega} \leq Ch^{2s} \|u\|_{1+s,\Omega},$$

$$(2.6) \quad |\lambda - \lambda_{\text{ECR}}| + \|u - u_{\text{ECR}}\|_{0,\Omega} + h^s \|\nabla_h(u - u_{\text{ECR}})\|_{0,\Omega} \leq Ch^{2s} \|u\|_{1+s,\Omega},$$

provided that $u \in H^{1+s}(\Omega, \mathbb{R}) \cap H_0^1(\Omega, \mathbb{R})$, $0 < s \leq 1$.

For the CR element and the ECR element, there holds the following commuting property of the canonical interpolations

$$(2.7) \quad \int_K \nabla(w - \Pi_{\text{CR}} w) \cdot \nabla v_h dx = 0 \quad \text{for any } w \in V, v_h \in V_{\text{CR}}, \\ \int_K \nabla(w - \Pi_{\text{ECR}} w) \cdot \nabla v_h dx = 0 \quad \text{for any } w \in V, v_h \in V_{\text{ECR}},$$

see [8, 9] for details.

2.3. Some Taylor expansions. On each element K , denote the centroid of element K by $\mathbf{M}_K = (M_1, M_2)$. Let $A_K = h^{-2} \sum_{i,j=1, i \neq j}^3 ((p_{i1} - p_{j1})^2 - (p_{i2} - p_{j2})^2)$, $B_K = h^{-2} \sum_{i=1}^3 (2p_{i1}p_{i2} - \sum_{j=1, j \neq i}^3 p_{i1}p_{j2})$, and $H_K = h^{-2} \sum_{i=1}^3 |e_i|^2$. We introduce three short-hand notations

$$\phi_{\text{ECR}}^1(\mathbf{x}) = (x_1 - M_1)^2 - (x_2 - M_2)^2, \quad \phi_{\text{ECR}}^2(\mathbf{x}) = (x_1 - M_1)(x_2 - M_2), \\ \phi_{\text{ECR}}^3(\mathbf{x}) = 2 - \frac{36}{h^2 H_K} \sum_{i=1}^2 (x_i - M_i)^2.$$

Note that functions ϕ_{ECR}^1 , ϕ_{ECR}^2 and ϕ_{ECR}^3 belong to the compliment space of the shape function space of the CR element with respect to $P_2(K)$.

For any element K and $H_h \in L^2(K, \mathbb{R}^{2 \times 2})$, define

$$\begin{aligned}
P_{P_1}^K(H_h) &= -\frac{1}{2} \sum_{i=1}^3 |e_i|^2 \phi_{i+1} \phi_{i-1} \|\mathbf{t}_i^T H_h \mathbf{t}_i\|_{0,K}, \\
P_{\text{CR}}^K(H_h) &= \frac{\|\mathbf{e}_1^T H_h \mathbf{e}_1 - \mathbf{e}_2^T H_h \mathbf{e}_2\|_{0,K}}{4|K|^{\frac{1}{2}}} (I - \Pi_{\text{ECR}}) \phi_{\text{ECR}}^1 + \frac{\|\mathbf{e}_1^T H_h \mathbf{e}_2\|_{0,K}}{|K|^{\frac{1}{2}}} (I - \Pi_{\text{ECR}}) \phi_{\text{ECR}}^2 \\
(2.8) \quad &\quad - \left(\frac{h^2(A_K + H_K)}{144|K|^{\frac{1}{2}}} \|\mathbf{e}_1^T H_h \mathbf{e}_1\|_{0,K} + \frac{h^2(H_K - A_K)}{144|K|^{\frac{1}{2}}} \|\mathbf{e}_2^T H_h \mathbf{e}_2\|_{0,K} \right. \\
&\quad \left. + \frac{h^2 B_K}{36|K|^{\frac{1}{2}}} \|\mathbf{e}_1^T H_h \mathbf{e}_2\|_{0,K} \right) \phi_{\text{ECR}}^3, \\
P_{\text{ECR}}^K(H_h) &= \frac{\|\mathbf{e}_1^T H_h \mathbf{e}_1 - \mathbf{e}_2^T H_h \mathbf{e}_2\|_{0,K}}{4|K|^{\frac{1}{2}}} (I - \Pi_{\text{ECR}}) \phi_{\text{ECR}}^1 + \frac{\|\mathbf{e}_1^T H_h \mathbf{e}_2\|_{0,K}}{|K|^{\frac{1}{2}}} (I - \Pi_{\text{ECR}}) \phi_{\text{ECR}}^2.
\end{aligned}$$

The following lemma lists the Taylor expansions of the canonical interpolation errors for the conforming linear element, the CR element and the ECR element, respectively. See [12, 15] for more details.

Lemma 2.1. *For any quadratic function $w \in P_2(K)$,*

$$\begin{aligned}
(I - \Pi_{P_1})w &= P_{P_1}^K(\nabla^2 w), \\
(2.9) \quad (I - \Pi_{\text{CR}})w &= P_{\text{CR}}^K(\nabla^2 w), \\
(I - \Pi_{\text{ECR}})w &= P_{\text{ECR}}^K(\nabla^2 w),
\end{aligned}$$

where ϕ_i the corresponding barycentric coordinate to vertex \mathbf{p}_i .

2.4. Superconvergence results for the CR element. Before designing a posteriori error estimators, we present the post-processing mechanism in [14] for the CR element. Denote the shape function space of the Raviart-Thomas element [19] by

$$\text{RT}_K := (P_0(K))^2 + \mathbf{x}P_0(K) \quad \text{for any } K \in \mathcal{T}_h,$$

and the corresponding finite element space by

$$\text{RT}(\mathcal{T}_h) := \{ \tau \in H(\text{div}, \Omega, \mathbb{R}^2) : \tau|_K \in \text{RT}_K \text{ for any } K \in \mathcal{T}_h \}.$$

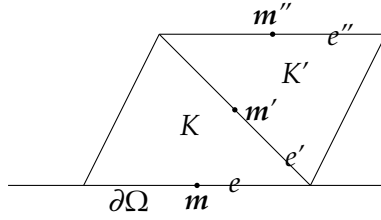
Given $\mathbf{q} \in \text{RT}(\mathcal{T}_h)$, define function $K_h \mathbf{q} \in V_{\text{CR}} \times V_{\text{CR}}$ as follows.

Definition 1. *1. For each interior edge $e \in \mathcal{E}_h^i$, the elements K_e^1 and K_e^2 are the pair of elements sharing e . Then the value of $K_h \mathbf{q}$ at the midpoint \mathbf{m}_e of e is*

$$K_h \mathbf{q}(\mathbf{m}_e) = \frac{1}{2} (q|_{K_e^1}(\mathbf{m}_e) + q|_{K_e^2}(\mathbf{m}_e)).$$

2. For each boundary edge $e \in \mathcal{E}_h^b$, let K be the element having e as an edge, and K' be an element sharing an edge $e' \in \mathcal{E}_h^i$ with K . Let e'' denote the edge of K' that does not intersect with e , and \mathbf{m} , \mathbf{m}' and \mathbf{m}'' be the midpoints of the edges e , e' and e'' , respectively. Then the value of $K_h \mathbf{q}$ at the point \mathbf{m} is

$$K_h \mathbf{q}(\mathbf{m}) = 2K_h \mathbf{q}(\mathbf{m}') - K_h \mathbf{q}(\mathbf{m}'').$$



A one order superconvergence of the CR element is analyzed in [13], that is

$$(2.10) \quad \|\nabla u - K_h \nabla_h u_{\text{CR}}\|_{0,\Omega} \leq Ch^2 |\ln h|^{1/2} |u|_{\frac{7}{2},\Omega},$$

provided that $u \in H^{\frac{7}{2}}(\Omega, \mathbb{R}) \cap H_0^1(\Omega, \mathbb{R})$. This superconvergence property leads to the following lemma for second order derivatives of eigenfunctions.

Lemma 2.2. *Let (λ, u) be the eigenpair of (2.1) with $u \in H^{\frac{7}{2}}(\Omega, \mathbb{R}) \cap H_0^1(\Omega, \mathbb{R})$, and $(\lambda_{\text{CR}}, u_{\text{CR}})$ be the corresponding approximate eigenpair of (2.2) in V_{CR} . It holds that*

$$\|\nabla^2 u - \nabla_h K_h \nabla_h u_{\text{CR}}\|_{0,\Omega} \leq Ch |\ln h|^{1/2} |u|_{\frac{7}{2},\Omega},$$

provided that $u \in H^{\frac{7}{2}}(\Omega, \mathbb{R}) \cap H_0^1(\Omega, \mathbb{R})$.

Proof. Let $\Pi_{P_2} u$ be the second order Lagrange interpolation of u , namely, the interpolation $\Pi_{P_2} u$ is a piecewise quadratic function over \mathcal{T}_h and admits the same value as u at the vertices of each element and the midpoint of each edge. It follows from the theory in [20] that

$$(2.11) \quad |u - \Pi_{P_2} u|_{i,\Omega} \leq Ch^{3-i} |u|_{3,\Omega}, \quad 0 \leq i \leq 2.$$

Due to the triangle inequality,

$$(2.12) \quad \|\nabla^2 u - \nabla_h K_h \nabla_h u_{\text{CR}}\|_{0,\Omega} \leq \|\nabla^2 u - \nabla_h^2 \Pi_{P_2} u\|_{0,\Omega} + \|\nabla_h^2 \Pi_{P_2} u - \nabla_h K_h \nabla_h u_{\text{CR}}\|_{0,\Omega}.$$

By the inverse inequality,

$$(2.13) \quad \|\nabla_h^2 \Pi_{P_2} u - \nabla_h K_h \nabla_h u_{\text{CR}}\|_{0,\Omega} \leq Ch^{-1} \|\nabla_h \Pi_{P_2} u - K_h \nabla_h u_{\text{CR}}\|_{0,\Omega}.$$

A combination of (2.10), (2.11) and (2.13) yields

$$(2.14) \quad \begin{aligned} \|\nabla_h^2 \Pi_{P_2} u - \nabla_h K_h \nabla_h u_{\text{CR}}\|_{0,\Omega} &\leq Ch^{-1} |\Pi_{P_2} u - u|_{1,\Omega} + h^{-1} \|\nabla u - K_h \nabla_h u_{\text{CR}}\|_{0,\Omega} \\ &\leq Ch |\ln h|^{1/2} |u|_{\frac{7}{2},\Omega}. \end{aligned}$$

A substitution of (2.11) and (2.14) into (2.12) concludes

$$\|\nabla^2 u - \nabla_h K_h \nabla_h u_{\text{CR}}\|_{0,\Omega} \leq Ch |\ln h|^{1/2} |u|_{\frac{7}{2},\Omega}$$

and completes the proof. \square

3. ASYMPTOTICALLY EXACT A POSTERIORI ERROR ESTIMATORS

In this section, asymptotically exact a posteriori error estimators of eigenvalues are designed and analyzed for the CR element and the ECR element.

For eigenvalues of the Laplacian operator solved by the conforming linear element, asymptotically exact a posteriori error estimators in [18] are based on a simple identity

$$\lambda_h - \lambda = |u - u_h|_{1,\Omega}^2 - \lambda \|u - u_h\|_{0,\Omega}^2,$$

where (λ_h, u_h) are discrete eigenpairs by this conforming element. Compared to the energy norm of errors of eigenfunctions, the error $\|u - u_h\|_{0,\Omega}$ is of higher order. By approximating the first term $|u - u_h|_{1,\Omega}^2$ with high accuracy gradient recovery techniques [16, 23, 26], asymptotically exact a posteriori error estimators of approximate eigenvalues are resulted following the above identity.

For nonconforming elements of second order elliptic eigenvalue problems, the corresponding identity includes an extra term, which represents consistency errors. Take the CR element for example,

$$(3.1) \quad \lambda - \lambda_{\text{CR}} = |u - u_{\text{CR}}|_{1,h}^2 + 2(a_h(u, u_{\text{CR}}) - \lambda_{\text{CR}}(u, u_{\text{CR}})) - \lambda_{\text{CR}} \|u - u_{\text{CR}}\|_{0,\Omega}^2.$$

The nonconformity leads to an extra term $a_h(u, u_{\text{CR}}) - \lambda_{\text{CR}}(u, u_{\text{CR}})$, which relates to values of eigenfunctions. Since there is no high accuracy techniques to recover eigenfunctions themselves, this extra term causes the difficulty to approximate discrete eigenvalues with high accuracy.

3.1. First type of asymptotically exact a posteriori error estimate. For both the CR element and the ECR element, the canonical interpolation admits a commuting property (2.7). By subtracting (2.7) from the extra term, the aforementioned consistency error can be expressed in terms of the interpolation errors of eigenfunctions. Taylor expansions in Lemma 2.1 imply that the main ingredients of interpolation errors are the second order derivatives of eigenfunctions. This important property turns the function recovery difficulty into a gradient recovery problem. To be specific, for the CR element, thanks to the commuting property (2.7) of the canonical interpolation operator Π_{CR} ,

$$(3.2) \quad \lambda - \lambda_{\text{CR}} = |u - u_{\text{CR}}|_{1,h}^2 - 2\lambda_{\text{CR}}(u - \Pi_{\text{CR}}u, u_{\text{CR}}) - \lambda_{\text{CR}} \|u - u_{\text{CR}}\|_{0,\Omega}^2.$$

The term $|u - u_{\text{CR}}|_{1,h}^2$ can be approximated with high accuracy by a direct application of gradient recovery techniques [16, 23, 26]. Thanks to the canonical interpolation and Lemma 2.1, the consistency error term is turned to an interpolation error term $(u - \Pi_{\text{CR}}u, u_{\text{CR}})$, which can be approximated with high accuracy by the use of these gradient recovery techniques. Then, asymptotically exact a posteriori error estimators of approximate eigenvalues are designed from the decomposition (3.2). This idea also works for eigenvalues by the ECR element.

Note that within each element K , both $\nabla_h K_h \nabla_h u_{\text{CR}}$ and $\nabla_h K_h \nabla_h u_{\text{ECR}}$ belong to $L^2(K, \mathbb{R}^{2 \times 2})$. Define the following a posteriori error estimators

$$(3.3) \quad F_{\text{CR},1}^{\text{CR}} = \|K_h \nabla_h u_{\text{CR}} - \nabla_h u_{\text{CR}}\|_{0,\Omega}^2 - 2\lambda_{\text{CR}} \sum_{K \in \mathcal{T}_h} \int_K P_{\text{CR}}^K(\nabla_h K_h \nabla_h u_{\text{CR}}) u_{\text{CR}} dx,$$

$$(3.4) \quad F_{\text{ECR},1}^{\text{ECR}} = \|K_h \nabla_h u_{\text{ECR}} - \nabla_h u_{\text{ECR}}\|_{0,\Omega}^2 - 2\lambda_{\text{ECR}} \sum_{K \in \mathcal{T}_h} \int_K P_{\text{ECR}}^K(\nabla_h K_h \nabla_h u_{\text{ECR}}) u_{\text{ECR}} dx$$

with the polynomials P_{CR}^K and P_{ECR}^K defined in (2.8).

Theorem 3.1. *Let (λ, u) be the eigenpairs of (2.1) with $u \in H^{\frac{7}{2}}(\Omega, \mathbb{R}) \cap H_0^1(\Omega, \mathbb{R})$, and $(\lambda_{\text{CR}}, u_{\text{CR}})$ be the corresponding approximate eigenpairs of (2.2) in V_{CR} . The a posteriori error estimators $F_{\text{CR},1}^{\text{CR}}$ in (3.3) satisfy*

$$|\lambda - \lambda_{\text{CR}} - F_{\text{CR},1}^{\text{CR}}| \leq Ch^3 |\ln h|^{1/2} |u|_{\frac{7}{2},\Omega}^2.$$

Proof. By the definition of $F_{\text{CR},1}^{\text{CR}}$ in (3.3) and (3.2),

$$(3.5) \quad \begin{aligned} \lambda - \lambda_{\text{CR}} - F_{\text{CR},1}^{\text{CR}} &= |u - u_{\text{CR}}|_{1,h}^2 - \|K_h \nabla_h u_{\text{CR}} - \nabla_h u_{\text{CR}}\|_{0,\Omega}^2 - \lambda_{\text{CR}} \|u - u_{\text{CR}}\|_{0,\Omega}^2 \\ &\quad - 2\lambda_{\text{CR}} \sum_{K \in \mathcal{T}_h} (u - \Pi_{\text{CR}} u - P_{\text{CR}}^K(\nabla^2 u), u_{\text{CR}})_{0,K} \\ &\quad - 2\lambda_{\text{CR}} \sum_{K \in \mathcal{T}_h} (P_{\text{CR}}^K(\nabla^2 u) - P_{\text{CR}}^K(\nabla_h K_h \nabla_h u_{\text{CR}}), u_{\text{CR}})_{0,K}. \end{aligned}$$

Thanks to (2.5) and (2.10),

$$(3.6) \quad \left| |u - u_{\text{CR}}|_{1,h}^2 - \|K_h \nabla_h u_{\text{CR}} - \nabla_h u_{\text{CR}}\|_{0,\Omega}^2 \right| \leq Ch^3 |\ln h|^{1/2} |u|_{\frac{7}{2},\Omega}^2.$$

A combination of the Bramble-Hilbert lemma and Lemma 2.1 leads to

$$(3.7) \quad \left| \sum_{K \in \mathcal{T}_h} (u - \Pi_{\text{CR}} u - P_{\text{CR}}^K(\nabla^2 u), u_{\text{CR}})_{0,K} \right| \leq Ch^3 |u|_{3,\Omega}.$$

By the definition of P_{CR}^K in (2.8) and Lemma 2.2,

$$(3.8) \quad \begin{aligned} &\left| \sum_{K \in \mathcal{T}_h} (P_{\text{CR}}^K(\nabla^2 u) - P_{\text{CR}}^K(\nabla_h K_h \nabla_h u_{\text{CR}}), u_{\text{CR}})_{0,K} \right| \\ &\leq C \sum_{K \in \mathcal{T}_h} h^2 \|\nabla^2 u - \nabla_h K_h \nabla_h u_{\text{CR}}\|_{0,K} \|u_{\text{CR}}\|_{0,K} \leq Ch^3 |\ln h|^{1/2} |u|_{\frac{7}{2},\Omega}^2. \end{aligned}$$

A substitution of (2.5), (3.6), (3.7) and (3.8) into (3.5) concludes

$$|\lambda - \lambda_{\text{CR}} - F_{\text{CR},1}^{\text{CR}}| \leq Ch^3 |\ln h|^{1/2} |u|_{\frac{7}{2},\Omega}^2$$

and completes the proof. \square \square

Notice that other a posteriori error estimators can be constructed following (3.3) with different recovered gradients from $K_h \nabla_h u_{\text{CR}}$. The resulting a posteriori error estimators are asymptotically exact as long as the recovered gradients superconverge to the gradients of eigenfunctions.

Similarly, the a posteriori error estimators $F_{\text{ECR},1}^{\text{ECR}}$ in (3.4) are also asymptotically exact as presented in the following theorem.

Theorem 3.2. *Let (λ, u) be the eigenpairs of (2.1) with $u \in H^{\frac{7}{2}}(\Omega, \mathbb{R}) \cap H_0^1(\Omega, \mathbb{R})$, and $(\lambda_{\text{ECR}}, u_{\text{ECR}})$ be the corresponding approximate eigenpairs of (2.2) in V_{ECR} . Then,*

$$|\lambda - \lambda_{\text{ECR}} - F_{\text{ECR},1}^{\text{ECR}}| \leq Ch^3 |\ln h|^{1/2} |u|_{\frac{7}{2}, \Omega}^2.$$

Remark 3.1. *Suppose that (λ, u) are the eigenpairs of the biharmonic operator with $u \in H^{\frac{9}{2}}(\Omega, \mathbb{R}) \cap H_0^2(\Omega, \mathbb{R})$, and $(\lambda_{\text{M}}, u_{\text{M}})$ are the corresponding approximate eigenpairs by the Morley element on a uniform triangulation \mathcal{T}_h . Thanks to the superconvergence of the Hellan–Herrmann–Johnson element and its equivalence to the Morley element, the recovered Hessian $K_h \nabla_h^2 u_{\text{M}}$ superconverges to $\nabla^2 u$. Since the canonical interpolation operator of the Morley element also admits the commuting property, a similar procedure produces asymptotically exact a posteriori error estimators for eigenvalues by the Morley element.*

3.2. Second type of asymptotically exact a posteriori error estimates. The second type of asymptotically exact a posteriori error estimate works for any nonconforming elements as long as the corresponding discrete space contains a conforming subspace and there exists some high accuracy gradient recovery technique for the elements.

The canonical interpolation of a conforming element is employed here to approximate the consistency error term. Take the CR element for example,

$$(3.9) \quad \lambda - \lambda_{\text{CR}} = |u - u_{\text{CR}}|_{1,h}^2 + 2a(u - \Pi_{\text{P}_1} u, u_{\text{CR}}) - 2\lambda_{\text{CR}}(u - \Pi_{\text{P}_1} u, u_{\text{CR}}) - \lambda_{\text{CR}} \|u - u_{\text{CR}}\|_{0,\Omega}^2,$$

and the canonical interpolation $\Pi_{\text{P}_1} u$ of the conforming linear element admits the same value of u on each vertex. The fact that this interpolation is not commutable, together with the discontinuity of recovered gradients, causes the failure of the same procedure as that for the first type of a posteriori error estimator. The main idea here is to rewrite the tricky term by the Green identity as follows.

$$(3.10) \quad a(u - \Pi_{\text{P}_1} u, u_{\text{CR}}) = \sum_{e \in \mathcal{E}_h} \int_e (u - \Pi_{\text{P}_1} u) \left[\frac{\partial u_{\text{CR}}}{\partial n} \right] ds.$$

On each interior edge, the interpolation error is approximated by the average of recovered interpolation errors on two adjacent elements.

Define the following a posteriori error estimators

$$(3.11) \quad \begin{aligned} F_{\text{CR},2}^{\text{CR}} = & \|K_h \nabla_h u_{\text{CR}} - \nabla_h u_{\text{CR}}\|_{0,\Omega}^2 + 2 \sum_{e \in \mathcal{E}_h} \int_e \{P_{\text{P}_1}^K(\nabla_h K_h \nabla_h u_{\text{CR}})\} \left[\frac{\partial u_{\text{CR}}}{\partial n} \right] ds \\ & - 2\lambda_{\text{CR}} \sum_{K \in \mathcal{T}_h} \int_K P_{\text{P}_1}^K(\nabla_h K_h \nabla_h u_{\text{CR}}) u_{\text{CR}} dx, \end{aligned}$$

$$\begin{aligned}
(3.12) \quad F_{\text{ECR},2}^{\text{ECR}} &= \|K_h \nabla_h u_{\text{ECR}} - \nabla_h u_{\text{ECR}}\|_{0,\Omega}^2 + 2 \sum_{e \in \mathcal{E}_h} \int_e \{P_{\text{P}_1}^K(\nabla_h K_h \nabla_h u_{\text{ECR}})\} \left[\frac{\partial u_{\text{ECR}}}{\partial n} \right] ds \\
&\quad - 2\lambda_{\text{ECR}} \sum_{K \in \mathcal{T}_h} \int_K P_{\text{P}_1}^K(\nabla_h K_h \nabla_h u_{\text{ECR}}) u_{\text{ECR}} dx,
\end{aligned}$$

with the polynomial $P_{\text{P}_1}^K$ defined in (2.8).

Theorem 3.3. *Let (λ, u) be the eigenpairs of (2.1) with $u \in H^{\frac{7}{2}}(\Omega, \mathbb{R}) \cap H_0^1(\Omega, \mathbb{R})$, and $(\lambda_{\text{CR}}, u_{\text{CR}})$ be the corresponding approximate eigenpairs of (2.2) in V_{CR} . The a posteriori error estimators $F_{\text{CR},2}^{\text{CR}}$ in (3.3) satisfy*

$$|\lambda - \lambda_{\text{CR}} - F_{\text{CR},2}^{\text{CR}}| \leq Ch^3 |\ln h|^{1/2} |u|_{\frac{7}{2},\Omega}^2.$$

Proof. According to the analysis for Theorem 3.1, the definition of $F_{\text{CR},2}^{\text{CR}}$, (3.9) and (3.10), it only remains to prove that

$$\left| \sum_{e \in \mathcal{E}_h} \int_e (u - \Pi_{\text{P}_1} u - \{P_{\text{P}_1}^K(\nabla_h K_h \nabla_h u_{\text{CR}})\}) \left[\frac{\partial u_{\text{CR}}}{\partial n} \right] ds \right| \leq Ch^3 |\ln h|^{1/2} |u|_{\frac{7}{2},\Omega}^2$$

The Cauchy-Schwarz inequality implies that

$$\begin{aligned}
(3.13) \quad &\int_e (u - \Pi_{\text{P}_1} u - \{P_{\text{P}_1}^K(\nabla_h K_h \nabla_h u_{\text{CR}})\}) \left[\frac{\partial u_{\text{CR}}}{\partial n} \right] ds \\
&\leq C \|u - \Pi_{\text{P}_1} u - \{P_{\text{P}_1}^K(\nabla_h K_h \nabla_h u_{\text{CR}})\}\|_{0,e} \left\| \left[\frac{\partial (u_{\text{CR}} - u)}{\partial n} \right] \right\|_{0,e}.
\end{aligned}$$

Due to the trace theorem and (2.5),

$$(3.14) \quad \left\| \left[\frac{\partial (u_{\text{CR}} - u)}{\partial n} \right] \right\|_{0,e} \leq Ch^{1/2} |u|_{2,\omega_e}.$$

According to the Bramble-Hilbert lemma, trace theorem and Lemma 2.1,

$$(3.15) \quad \|u - \Pi_{\text{P}_1} u - P_{\text{P}_1}^K(\nabla^2 u)\|_{0,e} \leq Ch^{5/2} |u|_{3,\omega_e}.$$

A combination of Lemma 2.2 and trace theorem gives

$$(3.16) \quad \|P_{\text{P}_1}^K(\nabla^2 u) - P_{\text{P}_1}^K(\nabla_h K_h \nabla_h u_{\text{CR}})\|_{0,e} \leq Ch^{5/2} |\ln h|^{1/2} |u|_{\frac{7}{2},\omega_e}.$$

A substitution of (3.14), (3.15) and (3.16) into (3.13) concludes

$$\left| \sum_{e \in \mathcal{E}_h} \int_e (u - \Pi_{\text{P}_1} u - \{P_{\text{P}_1}^K(\nabla_h K_h \nabla_h u_{\text{CR}})\}) \left[\frac{\partial u_{\text{CR}}}{\partial n} \right] ds \right| \leq Ch^3 |\ln h|^{1/2} |u|_{\frac{7}{2},\Omega}^2$$

and completes the proof. □ □

Similarly, the a posteriori error estimators $F_{\text{ECR},2}^{\text{ECR}}$ in (3.12) are also asymptotically exact. Note that other asymptotically exact a posteriori error estimators can be constructed following (3.11) and (3.12) but with different high accuracy recovered gradients.

Remark 3.2. *Since no commuting property of the element is required in the second design of asymptotically exact a posteriori error estimates, this error estimate applies for more general nonconforming elements and problems than the first type. Moreover, this type of a posteriori error estimate also works for higher order elliptic equations as long as this nonconforming element admits some superconvergence property and the discrete space contains some conforming subspace.*

4. POSTPROCESSING ALGORITHM

This section proposes two methods to improve accuracy of approximate eigenvalues by employing asymptotically exact a posteriori error estimators.

For the ease of presentation, we list the notations of different approximate eigenvalues and a posteriori error estimates here. Denote the approximate eigenpairs by the CR element, the ECR element and the conforming linear element on \mathcal{T}_h by $(\lambda_{\text{CR}}, u_{\text{CR}})$, $(\lambda_{\text{ECR}}, u_{\text{ECR}})$ and $(\lambda_{\text{P}_1}, u_{\text{P}_1})$, respectively. Apply the average-projection in [10] to the approximate eigenfunctions u_{CR} . Denote the resulting eigenfunctions by $\tilde{u}_{\text{P}_1^*}$. Define

$$(4.1) \quad u_{\text{P}_1^*} := \tilde{u}_{\text{P}_1^*} / \|\tilde{u}_{\text{P}_1^*}\|_{0,\Omega} \quad \text{and} \quad \lambda_{\text{P}_1^*} := a_h(u_{\text{P}_1^*}, u_{\text{P}_1^*}).$$

Denote the PPR postprocessing technique in [23] by the operator \bar{K}_h and

$$F_{\text{P}_1^*}^{\text{P}_1} := \|\bar{K}_h \nabla u_{\text{P}_1} - \nabla u_{\text{P}_1}\|_{0,\Omega}^2.$$

According to [18], $F_{\text{P}_1^*}^{\text{P}_1}$ are asymptotically exact a posteriori error estimates for eigenvalues λ_{P_1} . Replace the recovered gradient $\bar{K}_h \nabla u_{\text{P}_1}$ in the above definition by $K_h \nabla_h u_{\text{CR}}$ and $\bar{K}_h \nabla u_{\text{P}_1^*}$, and denote the resulting a posteriori error estimates by $F_{\text{P}_1^*}^{\text{CR}}$ and $F_{\text{P}_1^*}^{\text{P}_1^*}$, respectively. Lemma 2.2 reveals that error estimates $F_{\text{P}_1^*}^{\text{CR}}$ are asymptotically exact.

For eigenvalues λ_{CR} by the CR element, replace the recovered gradient $K_h \nabla_h u_{\text{CR}}$ in (3.3) by $\bar{K}_h \nabla u_{\text{P}_1}$ and $\bar{K}_h \nabla u_{\text{P}_1^*}$, and denote the resulting first type of a posteriori error estimators by $F_{\text{CR},1}^{\text{P}_1}$ and $F_{\text{CR},1}^{\text{P}_1^*}$, respectively. Similarly, replace the recovered gradient $K_h \nabla_h u_{\text{CR}}$ in (3.11) by $\bar{K}_h \nabla u_{\text{P}_1}$ and $\bar{K}_h \nabla u_{\text{P}_1^*}$, and denote the resulting second type of a posteriori error estimators by $F_{\text{CR},2}^{\text{P}_1}$ and $F_{\text{CR},2}^{\text{P}_1^*}$, respectively. According to [23], recovered gradients $\bar{K}_h \nabla u_{\text{P}_1}$ admit a similar superconvergence result as $K_h \nabla_h u_{\text{CR}}$ in (2.10). Thus, both error estimators $F_{\text{CR},1}^{\text{P}_1}$ and $F_{\text{CR},2}^{\text{P}_1}$ are asymptotically exact.

4.1. Recovered eigenvalues. The first approach is to add the discrete eigenvalues and the corresponding asymptotically exact a posteriori error estimates together. A direct application of Theorem 3.1 and 3.3 proves the higher accuracy of the resulting recovered eigenvalues than that of the original ones.

Table 1 lists the definitions of most recovered eigenvalues mentioned in this paper and the theoretical convergence rates for each recovered eigenvalue. These theoretical convergence rates are direct results from Theorem 3.1 and 3.3, and the superconvergence

	Recovered gradients	Recovered eigenvalues		order
λ_{CR}	$K_h \nabla_h u_{\text{CR}}$	$\lambda_{\text{CR},1}^{\text{R, CR}} := \lambda_{\text{CR}} + F_{\text{CR},1}^{\text{CR}}$	$\lambda_{\text{CR},2}^{\text{R, CR}} := \lambda_{\text{CR}} + F_{\text{CR},2}^{\text{CR}}$	3
	$\bar{K}_h \nabla u_{\text{P}_1}$	$\lambda_{\text{CR},1}^{\text{R, P}_1} := \lambda_{\text{CR}} + F_{\text{CR},1}^{\text{P}_1}$	$\lambda_{\text{CR},2}^{\text{R, P}_1} := \lambda_{\text{CR}} + F_{\text{CR},2}^{\text{P}_1}$	3
	$\bar{K}_h \nabla u_{\text{P}_1^*}$	$\lambda_{\text{CR},1}^{\text{R, P}_1^*} := \lambda_{\text{CR}} + F_{\text{CR},1}^{\text{P}_1^*}$	$\lambda_{\text{CR},2}^{\text{R, P}_1^*} := \lambda_{\text{CR}} + F_{\text{CR},2}^{\text{P}_1^*}$	-
λ_{P_1}	$K_h \nabla_h u_{\text{CR}}$	$\lambda_{\text{P}_1}^{\text{R, CR}} := \lambda_{\text{P}_1} + F_{\text{P}_1}^{\text{CR}}$		3
	$\bar{K}_h \nabla u_{\text{P}_1}$	$\lambda_{\text{P}_1}^{\text{R, P}_1} := \lambda_{\text{P}_1} + F_{\text{P}_1}^{\text{P}_1}$		3
	$\bar{K}_h \nabla u_{\text{P}_1^*}$	$\lambda_{\text{P}_1}^{\text{R, P}_1^*} := \lambda_{\text{P}_1} + F_{\text{P}_1}^{\text{P}_1^*}$		-
$\lambda_{\text{P}_1^*}$	$K_h \nabla_h u_{\text{CR}}$	$\lambda_{\text{P}_1^*}^{\text{R, CR}} := \lambda_{\text{P}_1^*} + F_{\text{P}_1^*}^{\text{CR}}$		3
	$\bar{K}_h \nabla u_{\text{P}_1}$	$\lambda_{\text{P}_1^*}^{\text{R, P}_1} := \lambda_{\text{P}_1^*} + F_{\text{P}_1^*}^{\text{P}_1}$		3
	$\bar{K}_h \nabla u_{\text{P}_1^*}$	$\lambda_{\text{P}_1^*}^{\text{R, P}_1^*} := \lambda_{\text{P}_1^*} + F_{\text{P}_1^*}^{\text{P}_1^*}$		-

TABLE 1. Definitions of recovered eigenvalues and the corresponding convergence rates.

results of the recovered gradients $K_h \nabla_h u_{\text{CR}}$ and $\bar{K}_h \nabla u_{\text{P}_1}$. Although there is no superconvergence result for the recovered gradient $\bar{K}_h \nabla u_{\text{P}_1^*}$, numerical examples still indicate a higher accuracy for the resulting recovered eigenvalues than the original ones.

4.2. Combining eigenvalues. Another way to achieve high accuracy is to take weighted-average of discrete eigenvalues with the weights computed by the corresponding asymptotically exact a posteriori error estimates. Usually the weighted-average of lower bounds, such as λ_{CR} and λ_{ECR} , and upper bounds, like λ_{P_1} and $\lambda_{\text{P}_1^*}$ can achieve better accuracy than those of two lower bounds or two upper bounds.

In this paper, the lower bounds of eigenvalues are fixed as λ_{CR} , and the upper bounds are λ_{P_1} or $\lambda_{\text{P}_1^*}$ as shown in Table 2. As listed in the first two columns of the table, four different asymptotically exact a posteriori error estimates $F_{\text{CR},1}^{\text{CR}}$, $F_{\text{CR},2}^{\text{CR}}$, $F_{\text{CR},1}^{\text{P}_1}$ and $F_{\text{CR},2}^{\text{P}_1}$ of lower bounds λ_{CR} are considered here to compute the weights. The first two rows list the two a posteriori error estimates $F_{\text{P}_1}^{\text{CR}}$ and $F_{\text{P}_1}^{\text{P}_1}$ for upper bounds λ_{P_1} , and the three a posteriori error estimates $F_{\text{P}_1^*}^{\text{CR}}$, $F_{\text{P}_1^*}^{\text{P}_1}$ and $F_{\text{P}_1^*}^{\text{P}_1^*}$ for upper bounds $\lambda_{\text{P}_1^*}$. The notations for the resulting combining eigenvalues are listed in the right bottom block of this table. Take the notation $\lambda_{\text{P}_1, \text{CR}, 1}^{\text{C, P}_1^*}$ for example. Define

$$(4.2) \quad \lambda_{\text{P}_1, \text{CR}, 1}^{\text{C, P}_1^*} := \frac{F_{\text{CR},1}^{\text{P}_1}}{F_{\text{CR},1}^{\text{P}_1} - F_{\text{P}_1^*}^{\text{CR}}} \lambda_{\text{P}_1^*} - \frac{F_{\text{P}_1^*}^{\text{CR}}}{F_{\text{CR},1}^{\text{P}_1} - F_{\text{P}_1^*}^{\text{CR}}} \lambda_{\text{CR}}.$$

The combining eigenvalues $\lambda_{\text{P}_1, \text{CR}, 1}^{\text{C, P}_1^*}$ are the weighted-average of the lower bounds λ_{CR} and upper bounds $\lambda_{\text{P}_1^*}$ with the weights computed from the a posteriori error estimates $F_{\text{CR},1}^{\text{P}_1}$ and $F_{\text{P}_1^*}^{\text{CR}}$. The other combining eigenvalues are defined in a similar way to the one in (4.2).

		λ_{P_1}		$\lambda_{P_1^*}$		
		$F_{P_1}^{CR}$	$F_{P_1}^{P_1}$	$F_{P_1^*}^{CR}$	$F_{P_1^*}^{P_1}$	$F_{P_1^*}^{P_1^*}$
λ_{CR}	$F_{CR,1}^{CR}$	$\lambda_{CR,CR,1}^{C, P_1}$	$\lambda_{CR,P_1,1}^{C, P_1}$	$\lambda_{CR,CR,1}^{C, P_1^*}$	$\lambda_{CR,P_1,1}^{C, P_1^*}$	$\lambda_{CR,P_1^*,1}^{C, P_1^*}$
	$F_{CR,2}^{CR}$	$\lambda_{CR,CR,2}^{C, P_1}$	$\lambda_{CR,P_1,2}^{C, P_1}$	$\lambda_{CR,CR,2}^{C, P_1^*}$	$\lambda_{CR,P_1,2}^{C, P_1^*}$	$\lambda_{CR,P_1^*,2}^{C, P_1^*}$
	$F_{CR,1}^{P_1}$	$\lambda_{P_1,CR,1}^{C, P_1}$	$\lambda_{P_1,P_1,1}^{C, P_1}$	$\lambda_{P_1,CR,1}^{C, P_1^*}$	$\lambda_{P_1,P_1,1}^{C, P_1^*}$	$\lambda_{P_1,P_1^*,1}^{C, P_1^*}$
	$F_{CR,2}^{P_1}$	$\lambda_{P_1,CR,2}^{C, P_1}$	$\lambda_{P_1,P_1,2}^{C, P_1}$	$\lambda_{P_1,CR,2}^{C, P_1^*}$	$\lambda_{P_1,P_1,2}^{C, P_1^*}$	$\lambda_{P_1,P_1^*,2}^{C, P_1^*}$

TABLE 2. Notations for varied combining eigenvalues.

The difference between the combining eigenvalues we propose and those in [11] lies in the design of approximate weights. In [11], two elements, which produce two upper bounds and two lower bounds of eigenvalues, respectively, are employed to solve eigenvalue problems on two successive meshes. The weights there are computed by the resulting four approximate eigenvalues, while the weights in this paper are computed by the corresponding a posteriori error estimators.

Most of the combining eigenvalues in Table 2 requires to solve two eigenvalue problems and the corresponding a posteriori error estimates, or even one more eigenvalue problem for the recovered gradient. The only exceptions are the combining eigenvalues $\lambda_{CR,CR,1}^{C, P_1^*}$, $\lambda_{CR,CR,2}^{C, P_1^*}$, $\lambda_{CR,P_1^*,1}^{C, P_1^*}$ and $\lambda_{CR,P_1^*,2}^{C, P_1^*}$, since the eigenpair $(\lambda_{P_1^*}, u_{P_1^*})$ are computed by the projection in [10] of nonconforming eigenfunctions u_{CR} . A third order convergence rate of the resulting combining eigenvalues $\lambda_{CR,CR,1}^{C, P_1^*}$ and $\lambda_{CR,CR,2}^{C, P_1^*}$ is guaranteed by the high accuracy recovered gradient $K_h \nabla_h u_{CR}$.

5. NUMERICAL EXAMPLES

This section presents six numerical tests for eigenvalues of the Laplacian operator. The first three examples deal with smooth enough eigenfunctions and the other three deal with singular eigenfunctions.

5.1. Adaptive algorithm. The a posteriori error estimators in Section 3 can also be employed to develop adaptive algorithms. Starting from an initial grid \mathcal{T}_1 , our adaptive mesh refinement process operates in the following (widely used) way (see [21]):

- (1) Set $k=0$.
- (2) Compute the eigenvalues from (2.2) on \mathcal{T}_k .
- (3) Compute the local error indicators. Take the CR element with the second type of asymptotically exact a posteriori error estimate for example. Define

$$(5.1) \quad \eta_K^2 = \|K_h \nabla_h u_{CR} - \nabla_h u_{CR}\|_{0,K}^2 + 2 \int_{\partial K} \{P_{P_1}^K(\nabla_h K_h \nabla_h u_{CR})\} \left[\frac{\partial u_{CR}}{\partial n} \right] ds - 2\lambda_{CR} \int_K P_{P_1}^K(\nabla_h K_h \nabla_h u_{CR}) u_{CR} dx,$$

- and $\eta^2 = \sum_{K \in \mathcal{T}} \eta_K^2$.
- (4) If η^2 is sufficiently small then stop. Otherwise, refine those elements $K \in \mathcal{T}_k$ with $\eta_K > \theta \max_{K \in \mathcal{T}_k} \eta_K$.
 - (5) Set $k = k + 1$ and go to (2).

Here $0 < \theta < 1$ is a fixed threshold. In our numerical experiments, we always set $\theta = 0.3$.

In this section, to distinguish from approximate eigenvalues on uniform triangulations, denote the approximate eigenvalue on those triangulations from the above adaptive algorithm by λ_{CR}^A , and the corresponding recovered eigenvalues by

$$\lambda_{CR}^{R,A} = \lambda_{CR}^A + F_{CR,2}^{CR}.$$

5.2. Example 1. In this example, the model problem (2.1) on the unit square $\Omega = (0, 1)^2$ is considered. The exact eigenvalues are

$$\lambda = (m^2 + n^2)\pi^2, \quad m, n \text{ are positive integers,}$$

and the corresponding eigenfunctions are $u = 2 \sin(m\pi x_1) \sin(n\pi x_2)$. The domain is partitioned by uniform triangles. The level one triangulation \mathcal{T}_1 consists of two right triangles, obtained by cutting the unit square with a north-east line. Each triangulation \mathcal{T}_i is refined into a half-sized triangulation uniformly, to get a higher level triangulation \mathcal{T}_{i+1} .

5.2.1. Recovered eigenvalues. Figure 1 plots the errors of the first approximate eigenvalues by the CR element, the ECR element, the conforming linear element and their corresponding recovered eigenvalues. It shows that the approximate eigenvalues λ_{CR} , λ_{ECR}

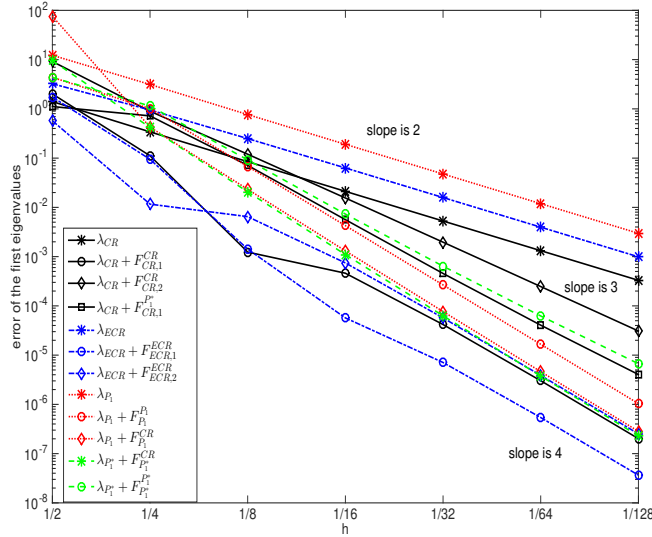


FIGURE 1. The errors of recovered eigenvalues for Example 1.

and λ_{P_1} converge at a rate 2, the recovered eigenvalues $\lambda_{CR,2}^{R,CR}$ converge at a rate 3 and

the recovered eigenvalues $\lambda_{CR,1}^{R,CR}$, $\lambda_{ECR,1}^{R,ECR}$, $\lambda_{ECR,2}^{R,ECR}$ and $\lambda_{P_1}^{R,P_1}$ converge at a higher rate 4. Note that although the theoretical convergence rates of the recovered eigenvalues $\lambda_{CR,1}^{R,CR}$, $\lambda_{ECR,1}^{R,ECR}$ and $\lambda_{ECR,2}^{R,ECR}$ are only 3, numerical tests indicate an even higher convergence rate 4. The errors of the recovered eigenvalues $\lambda_{CR,1}^{R,CR}$, $\lambda_{CR,2}^{R,CR}$, $\lambda_{ECR,1}^{R,ECR}$, $\lambda_{ECR,2}^{R,ECR}$ and $\lambda_{P_1}^{R,P_1}$ on \mathcal{T}_8 are 2.02×10^{-7} , 3.09×10^{-5} , 3.66×10^{-8} , 2.52×10^{-7} , 1.04×10^{-6} , respectively. They are significant improvements on the errors of the approximate eigenvalues λ_{CR} , λ_{ECR} and λ_{P_1} , which are 3.30×10^{-4} , 9.91×10^{-4} and 2.97×10^{-3} , respectively. This reveals that recovered eigenvalues are quite remarkable improvements on finite element solutions. It shows that the most accurate approximations are $\lambda_{ECR,1}^{R,ECR}$, followed by $\lambda_{ECR,1}^{R,ECR}$, $\lambda_{CR,2}^{R,CR}$, $\lambda_{P_1}^{R,CR}$ and $\lambda_{P_1}^{R,CR}$. Compared to approximations $\lambda_{P_1}^{R,CR}$, recovered eigenvalues $\lambda_{P_1}^{R,CR}$ achieve pretty much the same accuracy, but require to solve only discrete eigenvalue problem.

	$\lambda_{CR,CR,1}^{C,P_1}$	$\lambda_{CR,P_1,1}^{C,P_1}$	$\lambda_{CR,CR,1}^{C,P_1^*}$	$\lambda_{CR,P_1,1}^{C,P_1^*}$	$\lambda_{CR,P_1^*,1}^{C,P_1^*}$
error	9.95E-09	5.23E-09	1.03E-08	1.17E-09	6.50E-08
	$\lambda_{P_1,CR,1}^{C,P_1}$	$\lambda_{P_1,P_1,1}^{C,P_1}$	$\lambda_{P_1,CR,1}^{C,P_1^*}$	$\lambda_{P_1,P_1,1}^{C,P_1^*}$	$\lambda_{P_1,P_1^*,1}^{C,P_1^*}$
error	8.36E-08	7.89E-08	8.39E-08	7.48E-08	8.60E-09

TABLE 3. The errors of different combining eigenvalues on the mesh \mathcal{T}_8 for Example 1.

5.2.2. *Combining eigenvalues.* The errors of some combining eigenvalues on \mathcal{T}_8 are recorded in Table 3. Among all the errors in Table 3, the smallest one is 1.17×10^{-9} , and it is the error of a weighted-average of λ_{CR} and λ_{P_1} , where the weights are computed by $F_{CR,1}^{CR}$ and $F_{P_1}^{P_1}$. For the combining eigenvalue $\lambda_{CR,CR,1}^{C,P_1}$ on \mathcal{T}_8 , the error 1.03×10^{-8} is a little larger than the smallest one in Table 3, but less computational expense is required. Note that all these combining eigenvalues behave much better than the recovered eigenvalues $\lambda_{CR,1}^{R,CR}$, $\lambda_{P_1}^{R,P_1}$, $\lambda_{P_1}^{R,CR}$, $\lambda_{P_1^*}^{R,P_1}$ and $\lambda_{P_1^*}^{R,CR}$ in Figure 1.

5.2.3. *Extrapolation eigenvalues.* Table 4 compares the performance of recovered eigenvalues and extrapolation eigenvalues. It shows that the recovered eigenvalues $\lambda_{CR,1}^{R,CR}$ behave better than the extrapolation eigenvalues $\lambda_{P_1}^{EXP}$, but worse than λ_{CR}^{EXP} .

5.3. **Example 2: Neumann Boundary.** Next we consider the following eigenvalue problem (2.1) on the unit square $\Omega = (0, 1)^2$ with boundary conditions

$$u|_{x_1=0} = u|_{x_2=0} = u|_{x_2=1} = \partial_{x_1} u|_{x_1=1} = 0.$$

In this case, there exists an eigenpair (λ, u) where $\lambda = \frac{5\pi^2}{4}$, $u = 2 \cos \frac{\pi(x_1-1)}{2} \sin \pi x_2$.

We solve this problem on the same sequence of uniform triangulations employed in Example 1. Figure 2 shows that the approximate eigenvalues by the CR element, the ECR

h	λ_{CR}	λ_{P_1}	λ_{CR}^{EXP}	$\lambda_{P_1}^{EXP}$	$\lambda_{CR,1}^{R,CR}$	$\lambda_{P_1}^{R,P_1}$
1/4	-0.3407	3.1266	0.0140	0.0818	0.1236	1.0103
1/8	-8.47E-02	7.66E-01	6.42E-04	-2.04E-02	3.19E-03	6.77E-02
1/16	-2.11E-02	1.91E-01	3.72E-05	-1.34E-03	-4.20E-06	4.26E-03
1/32	-5.29E-03	4.76E-02	2.28E-06	-8.24E-05	-7.15E-06	2.66E-04
1/64	-1.32E-03	1.19E-02	1.42E-07	-5.12E-06	-6.65E-07	1.66E-05
1/128	-3.30E-04	2.97E-03	8.85E-09	-3.19E-07	-4.84E-08	1.04E-06
1/256	-8.26E-05	7.43E-04	5.59E-10	-1.99E-08	-3.25E-09	6.47E-08

TABLE 4. The errors of recovered eigenvalues and extrapolation eigenvalues, where $\lambda_{CR}^{EXP} = (4\lambda_{CR}^h - \lambda_{CR}^{2h})/3$ and $\lambda_{P_1}^{EXP} = (4\lambda_{P_1}^h - \lambda_{P_1}^{2h})/3$ are approximate eigenvalues by extrapolation methods.

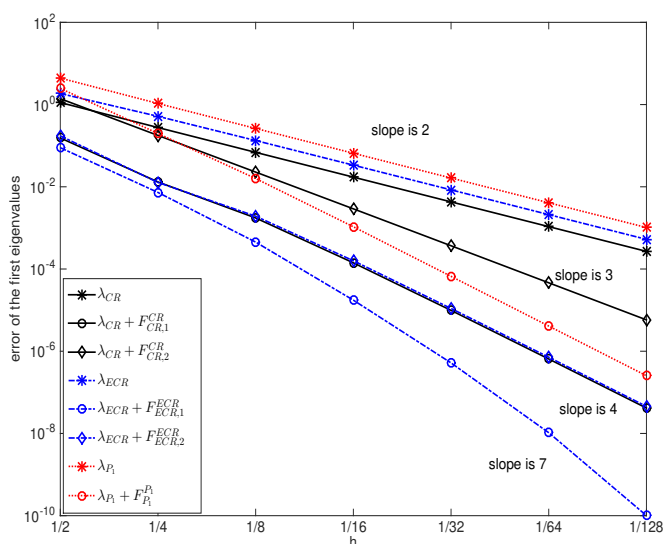


FIGURE 2. The errors of recovered eigenvalues for Example 2.

element and the conforming linear element converge at the same rate 2, the recovered eigenvalue $\lambda_{CR,2}^{R,CR}$ converges at a rate 3, the recovered eigenvalues $\lambda_{CR,1}^{R,CR}$, $\lambda_{ECR,2}^{R,ECR}$ and $\lambda_{P_1}^{R,P_1}$ converge at a rate 4. Especially, the recovered eigenvalue $\lambda_{ECR,1}^{R,ECR}$ converges at a strikingly higher rate 7.

5.4. Example 3: Triangle Domain. In this experiment, we consider the eigenvalue problem (2.1) on the domain which is an equilateral triangle:

$$\Omega = \{(x_1, x_2) \in \mathbb{R}^2 : 0 < x_2 < \sqrt{3}x_1, \sqrt{3}(1 - x_1) < x_2\}.$$

The boundary consists of three parts: $\Gamma_1 = \{(x_1, x_2) \in \mathbb{R}^2 : x_2 = \sqrt{3}x_1, 0.5 \leq x_1 \leq 1\}$, $\Gamma_2 = \{(x_1, x_2) \in \mathbb{R}^2 : x_2 = \sqrt{3}(1 - x_1), 0.5 \leq x_1 \leq 1\}$, $\Gamma_3 = \{(x_1, x_2) \in \mathbb{R}^2 : x_1 = 1, 0 \leq x_2 \leq 1\}$. Under the boundary conditions $u|_{\Gamma_1 \cup \Gamma_2} = 0$ and $\partial_{x_1} u|_{\Gamma_3} = 0$, there exists an eigenpair (λ, u) , where $\lambda = \frac{16\pi^2}{3}$ and

$$u = \frac{2\sqrt[4]{12}}{3} \left(\sin \frac{4\pi x_2}{\sqrt{3}} + \sin 2\pi(x_1 - \frac{x_2}{\sqrt{3}}) + \sin 2\pi(1 - x_1 - \frac{x_2}{\sqrt{3}}) \right).$$

The level one triangulation \mathcal{T}_1 is obtained by refining the domain Ω into four half-sized

	\mathcal{T}_2	\mathcal{T}_3	\mathcal{T}_4	\mathcal{T}_5	\mathcal{T}_6	\mathcal{T}_7
$\lambda - \lambda_{\text{CR}}$	-3.3545	3.6697	9.61E-01	2.43E-01	6.10E-02	1.53E-02
$\lambda - \lambda_{\text{CR}, 1}^{\text{R, CR}}$	-26.056	-2.10E-01	-9.46E-03	-2.80E-04	-6.08E-06	-8.80E-09
$\lambda - \lambda_{\text{CR}, 2}^{\text{R, CR}}$	-24.192	6.67E-01	1.11E-01	1.46E-02	1.81E-03	2.24E-04
$\lambda - \lambda_{\text{ECR}}$	1.177	4.8974	1.3186	3.36E-01	8.44E-02	2.11E-02
$\lambda - \lambda_{\text{ECR}, 1}^{\text{R, ECR}}$	-19.2136	0.3463	2.85E-02	2.27E-03	1.55E-04	1.01E-05
$\lambda - \lambda_{\text{ECR}, 2}^{\text{R, ECR}}$	-2.32E+01	2.12E-03	1.25E-04	3.48E-04	3.28E-05	2.40E-06
$\lambda - \lambda_{\text{P}_1}$	20.1024	-11.1936	-2.879	-7.29E-01	-1.83E-01	-4.58E-02
$\lambda - \lambda_{\text{P}_1}^{\text{R, P}_1}$	26.817	1.0209	0.1005	3.49E-03	9.62E-05	2.21E-06

TABLE 5. The errors and convergence rates of recovered eigenvalues for Example 3.

triangles. Each triangulation \mathcal{T}_i is refined into a half-sized triangulation uniformly, to get a higher level triangulation \mathcal{T}_{i+1} . It is showed in Table 5 that the recovered eigenvalues converge much faster than discrete eigenvalues and the recovered eigenvalue $\lambda_{\text{CR}, 1}^{\text{R, CR}}$ on \mathcal{T}_8 achieves the smallest error 8.80×10^{-9} .

5.5. Example 4: L-shaped Domain. Next we consider the eigenvalue problem (2.1) on a L-shaped domain $\Omega = (-1, 1)^2 / [0, 1] \times [-1, 0]$. For this problem, the third and the eighth eigenvalues are known to be $2\pi^2$ and $4\pi^2$, respectively, and the corresponding eigenfunctions are smooth.

In the computation, the level one triangulation is obtained by dividing the domain into three unit squares, each of which is further divided into two triangles. Each triangulation is refined into a half-sized triangulation uniformly to get a higher level triangulation. Since exact eigenvalues of this problem are unknown, we solve the first eight eigenvalues by the conforming P_3 element on the mesh \mathcal{T}_9 , and take them as reference eigenvalues.

	λ_1	λ_2	λ_3	λ_4	λ_5	λ_6	λ_7	λ_8
λ_{CR}	9.68E-04	9.65E-05	6.69E-05	1.79E-04	8.75E-04	7.75E-04	4.44E-04	3.48E-04
λ_{P_1}	-1.10E-03	-4.52E-04	-6.02E-04	-8.83E-04	-1.37E-03	-1.37E-03	-1.21E-03	-1.23E-03
$\lambda_{P_1^*}$	-1.41E-03	-4.53E-04	-6.03E-04	-8.85E-04	-1.60E-03	-1.51E-03	-1.21E-03	-1.32E-03
$\lambda_{CR,1}^{R,CR}$	4.22E-04	8.29E-07	-1.60E-07	-2.18E-07	3.11E-04	1.80E-04	1.11E-06	-8.53E-07
$\lambda_{CR,2}^{R,CR}$	2.41E-05	1.04E-05	8.32E-06	9.85E-06	2.48E-05	1.68E-05	1.70E-05	1.30E-05
$\lambda_{P_1}^{R,P_1}$	4.78E-04	7.24E-06	8.03E-07	3.35E-06	3.54E-04	2.09E-04	1.72E-05	4.11E-06
$\lambda_{P_1^*}^{R,P_1^*}$	7.53E-04	7.93E-06	2.46E-06	5.36E-06	5.62E-04	3.28E-04	1.84E-05	8.34E-06
$\lambda_{CR,P_1,2}^{C,P_1}$	1.94E-04	9.88E-06	7.65E-06	8.80E-06	1.34E-04	7.89E-05	1.70E-05	1.11E-05
$\lambda_{CR,P_1,2}^{C,P_1^*}$	2.46E-04	9.99E-06	7.80E-06	9.13E-06	1.76E-04	1.08E-04	1.73E-05	1.21E-05

TABLE 6. Relative errors of different approximations to the first eight eigenvalues on \mathcal{T}_7 for Example 4.

Table 6 compares the relative errors of the first eight approximate eigenvalues on \mathcal{T}_7 by different methods. It implies that the errors of the recovered eigenvalues $\lambda_{CR,1}^{R,CR}$ are slightly smaller than those of $\lambda_{P_1}^{R,P_1}$. For the first eigenvalue, the eigenfunction is singular. The corresponding recovered eigenvalues $\lambda_{CR,2}^{R,CR}$ achieve higher accuracy than the recovered eigenvalues $\lambda_{CR,1}^{R,CR}$ and $\lambda_{P_1}^{R,P_1}$. For the third eigenvalue, the corresponding eigenfunction is smooth. The relative errors of the third recovered eigenvalues $\lambda_{CR,1}^{R,CR}$ and $\lambda_{P_1}^{R,P_1}$ are 1.60×10^{-7} and 8.03×10^{-7} , respectively, smaller than those of the recovered eigenvalues $\lambda_{CR,2}^{R,CR}$.

It is observed in Table 6 that for different eigenvalues, the relative errors of the approximate eigenvalues λ_{CR} do not vary too much. This phenomenon still holds for the approximate eigenvalues λ_{P_1} and $\lambda_{P_1^*}$. However, for the approximate eigenvalues $\lambda_{CR,1}^{R,CR}$, $\lambda_{P_1}^{R,P_1}$ and $\lambda_{P_1^*}^{R,P_1^*}$, the relative errors of various eigenvalues are quite different. The reason is that the accuracy of the first type of a posteriori error estimators relies heavily on the regularity of the corresponding eigenfunctions. The relative errors of the various recovered eigenvalues $\lambda_{CR,2}^{R,CR}$ differ little from each other. This fact implies that the accuracy of the second type of a posteriori error estimators is insensitive to the regularity of eigenfunctions.

Figure 3 plots the resulting eigenfunctions on triangulations \mathcal{T}_{10} , \mathcal{T}_{20} , \mathcal{T}_{30} and \mathcal{T}_{40} from the adaptive algorithm in Section 5.1. Figure 4 plots the relationship between errors of the first eigenvalues and the size of discrete eigenvalue problems. It shows that approximate eigenvalues λ_{CR}^A on adaptive triangulations behave even better than the first type of recovered eigenvalues $\lambda_{CR,1}^{R,CR}$ on uniform triangulations. The recovered eigenvalues $\lambda_{CR,2}^{R,CR}$ on the uniform triangulations behave best among all approximations.

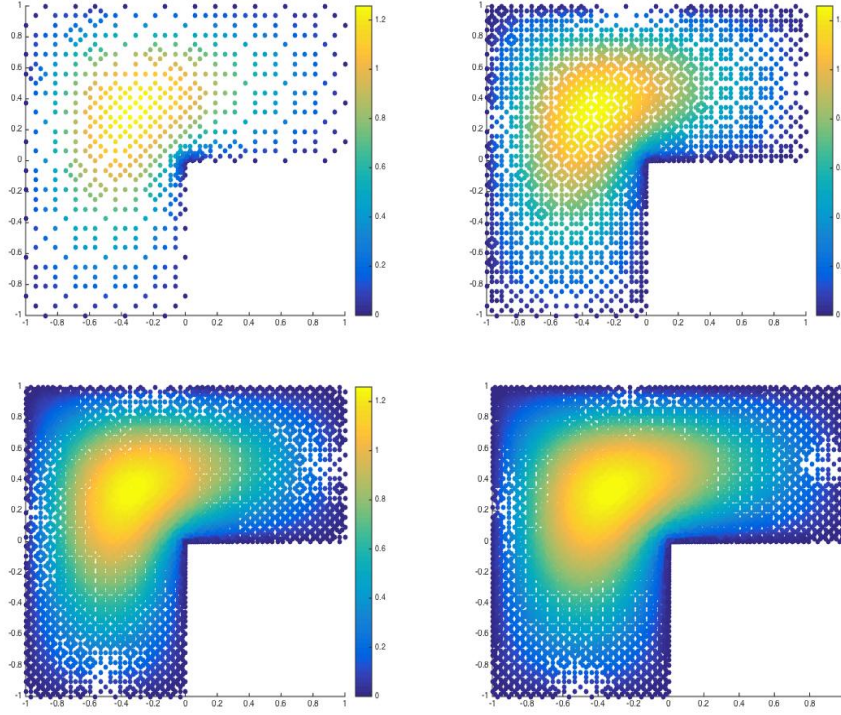


FIGURE 3. The first eigenfunctions on adaptive triangulations with $k = 10$, $k = 20$, $k = 30$ and $k = 40$ for Example 4.

5.6. **Example 5: H-shaped Domain.** Next we consider the following eigenvalue problem

$$(5.2) \quad \begin{aligned} -\Delta u &= \lambda u & \text{in } \Omega, \\ u &= 0 & \text{in } \partial\Omega, \end{aligned}$$

on a H-shaped domain in Figure 5. Note that the first eigenfunction is singular.

The level one triangulation is uniform and shown in Figure 5. Each triangulation is refined into a half-sized triangulation uniformly to get a higher level triangulation. Since exact eigenvalues of this problem are unknown, the conforming P_3 element is employed to solve the eigenvalue problem on the mesh \mathcal{T}_9 , and the resulting approximate eigenvalues are taken as reference eigenvalues.

As presented in Table 7, the recovered eigenvalues $\lambda_{CR,2}^{R,CR}$ performs better than $\lambda_{CR,1}^{R,CR}$ when the eigenfunctions are singular. The errors of $\lambda_{CR,1}^{R,CR}$ and $\lambda_{CR,2}^{R,CR}$ on \mathcal{T}_7 are 2.06×10^{-5} and 4.56×10^{-3} , respectively. The recovered eigenvalue $\lambda_{CR,2}^{R,CR}$ on \mathcal{T}_7 achieves the smallest error, remarkably smaller than the combining eigenvalues with error 1.48×10^{-3} . The reason why the combining eigenvalues behave worse is that the asymptotically exact a posteriori error estimators $F_{P_1}^{CR}$ are less accurate than $F_{CR,2}^{CR}$ when the eigenfunctions are singular.

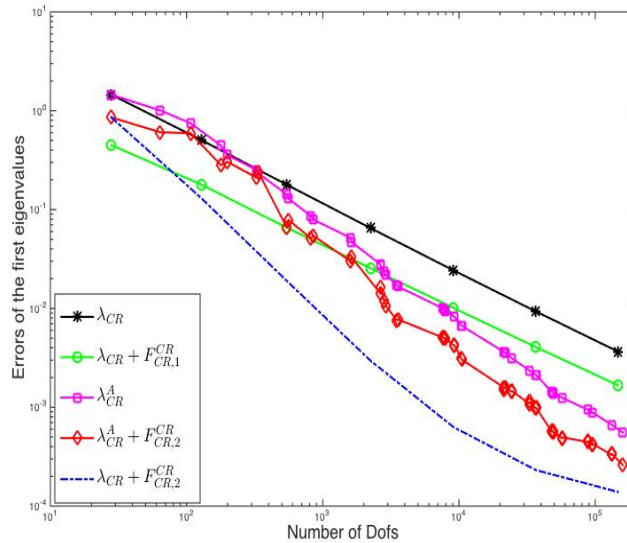


FIGURE 4. The errors of the first eigenvalue for Example 4.

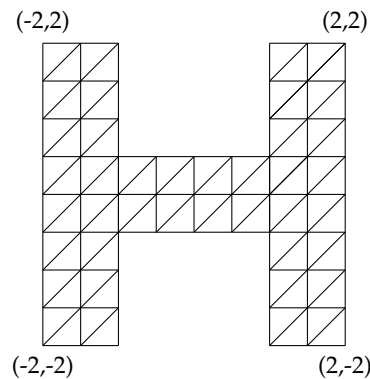
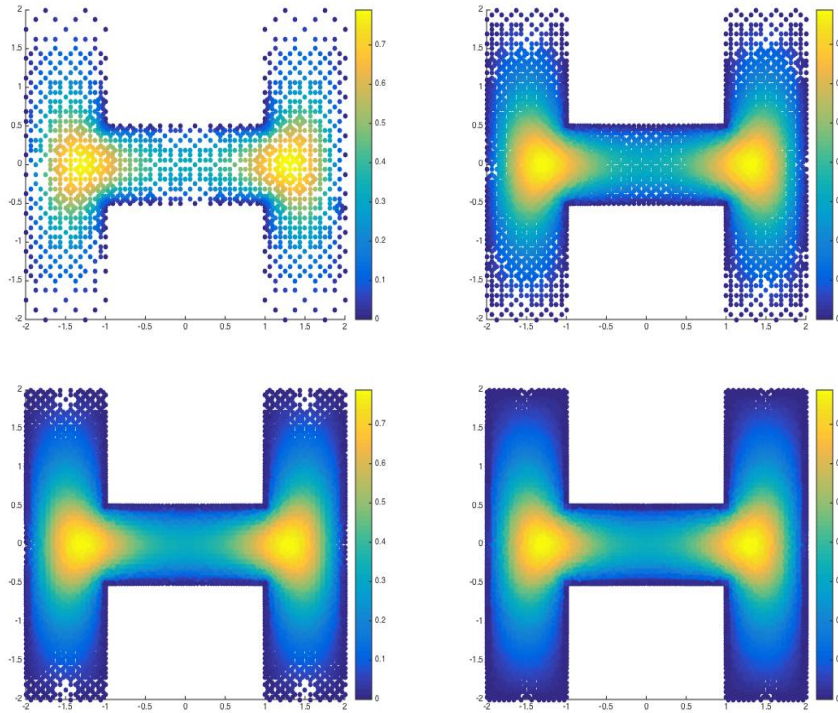


FIGURE 5. Initial triangulation for Example 5.

Figure 6 plots the resulting eigenfunctions on triangulations \mathcal{T}_{10} , \mathcal{T}_{20} , \mathcal{T}_{30} and \mathcal{T}_{40} from the adaptive algorithm in Section 5.1. Figure 7 plots the relationship between errors of the first eigenvalues and the size of discrete eigenvalue problems. The performance of these approximations is quite similar to that for Example 4. Compared to the first type of recovered eigenvalues $\lambda_{CR,1}^{R,CR}$ on uniform triangulations, approximate eigenvalues λ_{CR}^A on adaptive triangulations achieve higher accuracy. The recovered eigenvalues $\lambda_{CR}^{R,A}$ on adaptive triangulations behave much better than other approximations.

h	λ_{CR}	λ_{P_1}	$\lambda_{\text{CR},1}^{\text{R,CR}}$	$\lambda_{\text{CR},2}^{\text{R,CR}}$	$\lambda_{P_1}^{\text{R},P_1}$	$\lambda_{P_1^*}^{\text{R},P_1^*}$	$\lambda_{\text{CR},\text{CR},2}^{\text{C},P_1^*}$
\mathcal{T}_2	1.61E+00	-2.84E+00	6.27E-01	4.39E-01	1.93E+00	2.01E+00	6.46E-01
\mathcal{T}_3	5.74E-01	-7.99E-01	2.05E-01	6.03E-02	3.37E-01	4.70E-01	1.21E-01
\mathcal{T}_4	2.06E-01	-2.54E-01	7.52E-02	8.46E-03	8.76E-02	1.44E-01	3.07E-02
\mathcal{T}_5	7.54E-02	-8.68E-02	2.91E-02	9.72E-04	3.04E-02	5.26E-02	1.00E-02
\mathcal{T}_6	2.83E-02	-3.10E-02	1.15E-02	8.95E-05	1.17E-02	2.05E-02	3.74E-03
\mathcal{T}_7	1.09E-02	-1.15E-02	4.56E-03	2.06E-05	4.61E-03	8.10E-03	1.48E-03

TABLE 7. Errors of the first eigenvalue approximations by different methods for Example 5.

FIGURE 6. The first eigenfunctions on adaptive triangulations with $k = 10$, $k = 20$, $k = 30$ and $k = 40$ for Example 5.

5.7. Example 6: Hollow-shaped Domain. Next we consider the following eigenvalue problem

$$(5.3) \quad \begin{aligned} -\Delta u &= \lambda u & \text{in } \Omega, \\ u &= 0 & \text{in } \partial\Omega, \end{aligned}$$

on a hollow-shaped domain in Figure 8. Note that the first eigenfunction is singular.

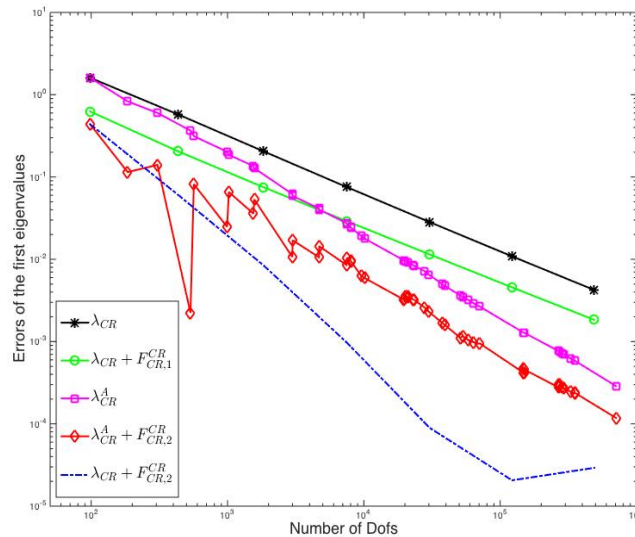


FIGURE 7. The errors of the first eigenvalue for Example 5.

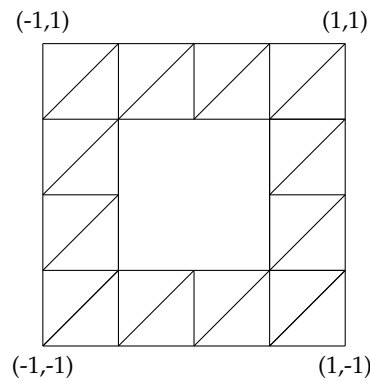


FIGURE 8. Initial triangulation for Example 6.

The level one triangulation is uniform and shown in Figure 8. Each triangulation is refined into a half-sized triangulation uniformly to get a higher level triangulation. Since exact eigenvalues of this problem are unknown, the conforming P_3 element is employed to solve the eigenvalue problem on the mesh \mathcal{T}_9 , and the resulting approximate eigenvalues are taken as reference eigenvalues.

Table 8 lists the errors of approximate eigenvalues on each mesh by different methods. The recovered eigenvalues $\lambda_{CR,2}^{R,CR}$ performs remarkably better than all the other recovered eigenvalues and combining eigenvalues when the eigenfunctions are singular. The error

h	λ_{CR}	λ_{P_1}	$\lambda_{CR,1}^{R,CR}$	$\lambda_{CR,2}^{R,CR}$	$\lambda_{P_1}^{R,P_1}$	$\lambda_{P_1}^{R,P_1^*}$	$\lambda_{P_1^*,P_1^*,2}^{C,P_1^*}$
\mathcal{T}_2	6.12E+00	-1.10E+01	1.41E+00	1.21E+00	7.25E+00	7.84E+00	-3.11E-01
\mathcal{T}_3	1.97E+00	-2.99E+00	4.87E-01	1.34E-01	1.07E+00	1.53E+00	-5.25E-02
\mathcal{T}_4	6.54E-01	-8.91E-01	1.91E-01	1.73E-02	2.41E-01	4.01E-01	-1.78E-02
\mathcal{T}_5	2.26E-01	-2.84E-01	7.53E-02	1.33E-03	8.00E-02	1.40E-01	-5.85E-03
\mathcal{T}_6	8.15E-02	-9.56E-02	2.99E-02	-3.15E-05	3.06E-02	5.39E-02	-1.71E-03
\mathcal{T}_7	3.03E-02	-3.36E-02	1.20E-02	2.47E-06	1.21E-02	2.13E-02	-4.37E-04

TABLE 8. Errors of the first eigenvalue approximations by different methods for Example 6.

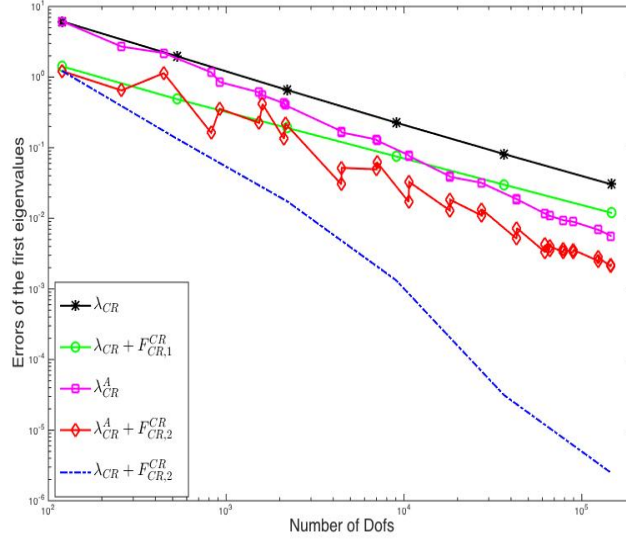


FIGURE 9. The errors of the first eigenvalue for Example 6.

of the recovered eigenvalue $\lambda_{CR, P_1^*, 2}^{C, P_1^*}$ on \mathcal{T}_7 is 4.37×10^{-4} , it is smaller than all the other approximations but $\lambda_{CR, 2}^{R, CR}$. It implies that if eigenfunctions are not smooth enough, the second type of asymptotically exact a posteriori error estimates $F_{CR, 2}^{CR}$ for the corresponding eigenvalues admit higher accuracy than $F_{CR, 1}^{CR}$.

Figure 9 plots the relationship between errors of the first eigenvalues and the size of discrete eigenvalue problems. Figure 10 plots the resulting eigenfunctions on triangulations \mathcal{T}_{10} , \mathcal{T}_{20} , \mathcal{T}_{30} and \mathcal{T}_{40} from the adaptive algorithm in Section 5.1. The performance of these approximations is quite similar to those for Example 4 and Example 5. The second type of recovered eigenvalues on uniform triangulations achieve remarkable higher accuracy of eigenvalues than all the other approximations.

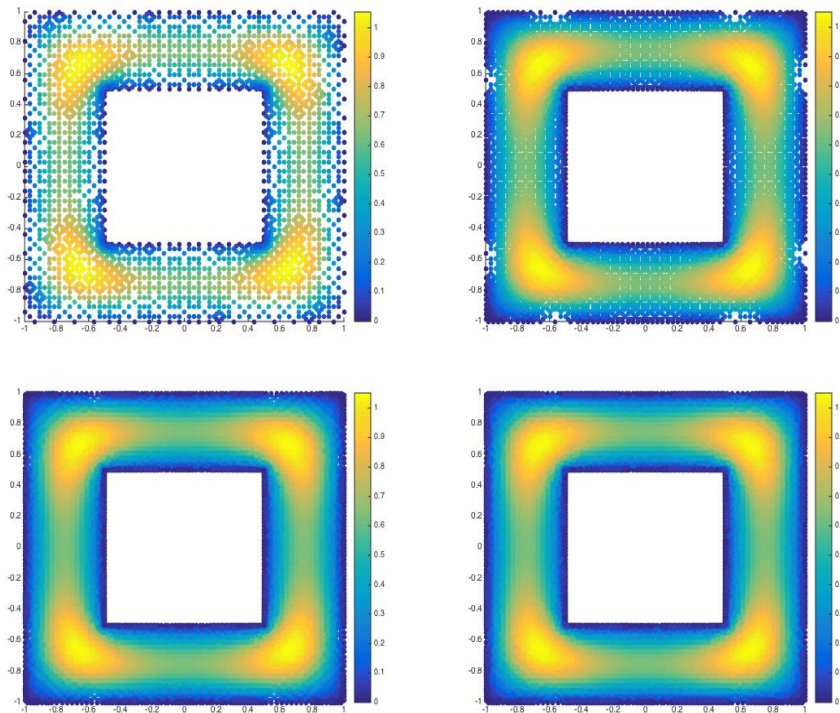


FIGURE 10. The first eigenfunctions on adaptive triangulations with $k = 10$, $k = 20$, $k = 30$ and $k = 40$ for Example 6.

REFERENCES

- [1] Mark Ainsworth and J Tinsley Oden. *A posteriori error estimation in finite element analysis*, volume 37. John Wiley & Sons, 2011.
- [2] Ivo Babuška and Werner C Rheinboldt. A-posteriori error estimates for the finite element method. *International Journal for Numerical Methods in Engineering*, 12(10):1597–1615, 1978.
- [3] Ivo Babuška, T Strouboulis, CS Upadhyay, SK Gangaraj, and K Copps. Validation of a posteriori error estimators by numerical approach. *International journal for numerical methods in engineering*, 37(7):1073–1123, 1994.
- [4] Roland Becker, Shipeng Mao, and Zhongci Shi. A convergent nonconforming adaptive finite element method with quasi-optimal complexity. *SIAM Journal on Numerical Analysis*, 47(6):4639–4659, 2010.
- [5] Carsten Carstensen. All first-order averaging techniques for a posteriori finite element error control on unstructured grids are efficient and reliable. *Mathematics of Computation*, 73(247):1153–1165, 2004.
- [6] Carsten Carstensen and Jun Hu. A unifying theory of a posteriori error control for nonconforming finite element methods. *Numerische Mathematik*, 107(3):473–502, 2007.

- [7] Carsten Carstensen, Jun Hu, and Antonio Orlando. Framework for the a posteriori error analysis of nonconforming finite elements. *SIAM Journal on Numerical Analysis*, 45(1):68–82, 2007.
- [8] Michel Crouzeix and Pierre-Arnaud Raviart. Conforming and nonconforming finite element methods for solving the stationary Stokes equations. *Revue française d'automatique informatique recherche opérationnelle. Mathématique*, 7(R3):33–75, 1973.
- [9] Jun Hu, Yunqing Huang, and Qun Lin. Lower bounds for eigenvalues of elliptic operators: By nonconforming finite element methods. *Journal of Scientific Computing*, 61(1):196–221, 2014.
- [10] Jun Hu, Yunqing Huang, and Quan Shen. Constructing both lower and upper bounds for the eigenvalues of elliptic operators by nonconforming finite element methods. *Numerische Mathematik*, 131(2):273–302, 2015.
- [11] Jun Hu, Yunqing Huang, and Qun Shen. A high accuracy post-processing algorithm for the eigenvalues of elliptic operators. *Journal of Scientific Computing*, 52(2):426–445, 2012.
- [12] Jun Hu and Limin Ma. Asymptotic expansions of eigenvalues by both the crouzeix-raviart and enriched crouzeix-raviart elements. *arXiv preprint arXiv:1902.09524*, 2019.
- [13] Jun Hu, Limin Ma, and Rui Ma. Optimal superconvergence analysis for the Crouzeix-Raviart and the Morley elements. *arXiv preprint arXiv:1808.09810*, 2018.
- [14] Jun Hu and Rui Ma. Superconvergence of both the Crouzeix-Raviart and Morley elements. *Numerische Mathematik*, 132(3):491–509, 2016.
- [15] Yunqing Huang and Jinchao Xu. Superconvergence of quadratic finite elements on mildly structured grids. *Mathematics of computation*, 77(263):1253–1268, 2008.
- [16] Yunqing Huang and Nianyu Yi. The superconvergent cluster recovery method. *Journal of Scientific Computing*, 44(3):301–322, 2010.
- [17] Qun Lin and Aihui Zhou. Notes on superconvergence and its related topics. *Journal of Computational Mathematics*, pages 211–214, 1993.
- [18] Ahmed Naga, Zhimin Zhang, and Aihui Zhou. Enhancing eigenvalue approximation by gradient recovery. *Journal of Scientific Computing*, (28):1289–1300, 2006.
- [19] Pierre-Arnaud Raviart and Jean-Marie Thomas. A mixed finite element method for second order elliptic problems. *Springer Berlin Heidelberg*, (606):292–315, 1977.
- [20] Zhong-Ci Shi and Ming Wang. The finite element method(In Chinese). *Science Press, Beijing*, 2010.
- [21] Rüdiger Verfürth. A review of a posteriori error estimation and adaptive meshrefinement techniques. *Wiley-Teubner, London, UK*, 1996.
- [22] Ningning Yan and Aihui Zhou. Gradient recovery type a posteriori error estimates for finite element approximations on irregular meshes. *Computer methods in applied mechanics and engineering*, 190(32-33):4289–4299, 2001.
- [23] Zhimin Zhang. A posteriori error estimates based on the polynomial preserving recovery. *Siam Journal on Numerical Analysis*, 42(4):1780–1800, 2005.
- [24] Zhimin Zhang and Ahmed Naga. A new finite element gradient recovery method: superconvergence property. *SIAM Journal on Scientific Computing*, 26(4):1192–1213, 2005.

-
- [25] Olgierd Cecil Zienkiewicz and Jianzhong Zhu. The superconvergent patch recovery and a posteriori error estimates. part 1: The recovery technique. *International Journal for Numerical Methods in Engineering*, 33(7):1331–1364, 1992.
- [26] Olgierd Cecil Zienkiewicz and Jianzhong Zhu. The superconvergent patch recovery and a posteriori error estimates. part ii: Error estimates and adaptivity. *International Journal for Numerical Methods in Engineering*, 33(7):1331–1364, 1992.

LMAM AND SCHOOL OF MATHEMATICAL SCIENCES, PEKING UNIVERSITY, BEIJING 100871, P. R. CHINA. HUN@MATH.PKU.EDU.CN

LMAM AND SCHOOL OF MATHEMATICAL SCIENCES, PEKING UNIVERSITY, BEIJING 100871, P. R. CHINA. MALIM-INPKU@GMAIL.COM